

This work was written as part of one of the author's official duties as an Employee of the United States Government and is therefore a work of the United States Government. In accordance with 17 U.S.C. 105, no copyright protection is available for such works under U.S. Law.

Public Domain Mark 1.0

<https://creativecommons.org/publicdomain/mark/1.0/>

Access to this work was provided by the University of Maryland, Baltimore County (UMBC) ScholarWorks@UMBC digital repository on the Maryland Shared Open Access (MD-SOAR) platform.

Please provide feedback

Please support the ScholarWorks@UMBC repository by emailing scholarworks-group@umbc.edu and telling us what having access to this work means to you and why it's important to you. Thank you.



Development of an operational land water mask for MODIS Collection 6, and influence on downstream data products

M. L. Carroll, C. M. DiMiceli, J. R. G. Townshend, R. A. Sohlberg, A. I. Elders, S. Devadiga, A. M. Sayer & R. C. Levy

To cite this article: M. L. Carroll, C. M. DiMiceli, J. R. G. Townshend, R. A. Sohlberg, A. I. Elders, S. Devadiga, A. M. Sayer & R. C. Levy (2017) Development of an operational land water mask for MODIS Collection 6, and influence on downstream data products, International Journal of Digital Earth, 10:2, 207-218, DOI: [10.1080/17538947.2016.1232756](https://doi.org/10.1080/17538947.2016.1232756)

To link to this article: <https://doi.org/10.1080/17538947.2016.1232756>



Published online: 04 Oct 2016.



Submit your article to this journal [↗](#)



Article views: 751



View related articles [↗](#)





View Crossmark data [↗](#)



Citing articles: 10 View citing articles [↗](#)



Development of an operational land water mask for MODIS Collection 6, and influence on downstream data products

M. L. Carroll^{a,b}, C. M. DiMiceli^c, J. R. G. Townshend^c, R. A. Sohlberg^c, A. I. Elders^d , S. Devadiga^{b,e} , A. M. Sayer^{f,g} and R. C. Levy^g

^aNASA/GSFC Biospheric Sciences Laboratory, Greenbelt, MD, USA; ^bScience Systems and Applications Inc., Lanham, MD, USA; ^cDepartment of Geographical Sciences, University of Maryland, College Park, MD, USA; ^dAtmospheric, Oceanic and Earth Sciences, George Mason University, Fairfax, VA, USA; ^eNASA/GSFC Terrestrial Information Systems Laboratory, Greenbelt, MD, USA; ^fGoddard Earth Sciences Technology and Research, Universities Space Research Association, Greenbelt, MD, USA; ^gNASA/GSFC Climate and Radiation Laboratory, Greenbelt, MD, USA

ABSTRACT

Data from the Moderate Resolution Imaging Spectro-radiometer (MODIS) on-board the Earth Observing System Terra and Aqua satellites are processed using a land water mask to determine when an algorithm no longer needs to be run or when an algorithm needs to follow a different pathway. Entering the fourth reprocessing (Collection 6 (C6)) the MODIS team replaced the 1 km water mask with a 500 m water mask for improved representation of the continental surfaces. The new water mask represents more small water bodies for an overall increase in water surface from 1% to 2% of the continental surface. While this is still a small fraction of the overall global surface area the increase is more dramatic in certain areas such as the Arctic and Boreal regions where there are dramatic increases in water surface area in the new mask. MODIS products generated by the on-going C6 reprocessing using the new land water mask show significant impact in areas with high concentrations of change in the land water mask. Here differences between the Collection 5 (C5) and C6 water masks and the impact of these differences on the MOD04 aerosol product and the MOD11 land surface temperature product are shown.

ARTICLE HISTORY

Received 22 June 2016

Accepted 31 August 2016

KEYWORDS

Earth observation; image processing; land cover; remote sensing; water resources

1. Introduction

Data from the Moderate Resolution Imaging Spectro-radiometer (MODIS) are processed from Level 0 (raw uncalibrated instrument measurements) to Level 4 (calibrated radiances, and derived products) at the MODIS Adaptive Processing System at the NASA Goddard Space Flight Center. There are over 100 algorithms in thematic areas of Land, Oceans, and Atmospheres that are processed. Some of these algorithms use a land/water mask to achieve greater accuracy in the physical measurements (e.g. land surface temperature (LST), aerosol retrievals, cloud detection, etc.) (Justice et al. 2002; Masuoka et al. 2011). The land/water mask that was used from launch through Collection 3 had a spatial resolution of 1 km and was derived from the Advanced Very High Resolution Radiometer land cover product (1996), GTOPO30, and other common resources at the time. This product was determined by the MODIS Land team to have inaccuracies that caused errors to propagate into downstream data products and was replaced prior to the start of the second reprocessing (Collection 4 (C4)) in 2004. The C4 water mask, generated by the MODIS Land Cover team at Boston University (Salomon et al. 2004), was still at 1 km spatial resolution but improved on some of the gross

misplacement of rivers (Carroll et al. 2009) that were causing known problems in MODIS data products. During subsequent MODIS Land science team meetings in 2005–2008, the team expressed an interest in further improving the land/water mask with finer resolution products in order to produce more continuous rivers and better define the lakes and coastlines. A team from the University of Maryland led an effort from 2008 to 2009 to create a new global 250 m land/water mask for use in future reprocessing of MODIS data products. The 250 m water mask was completed and released to the public in August 2009 (Carroll et al. 2009).

The global 250 m water map is a binary depiction of the Earth’s surface as either land or water. Prior water masks used in MODIS processing further defined the water into the classes shown in Table 1. The MODIS Land team decided that the most appropriate configuration for the new Collection 6 (C6) land/water mask would be to maintain the categories shown in Table 1 and produce a product at 500 m spatial resolution to match the spatial resolution of the majority of the MODIS land products. The team from the University of Maryland accepted this task in June 2010 and completed the project in September 2010. Here, we present the methods used to convert the binary mask to a categorical representation consistent with prior collections, describe the differences between the C4/5 and C6 masks, and identify specific impacts of this difference on the MOD04 aerosol and MOD11 LST.

2. Methods

The base product used in the development of the operational land/water mask for C6 MODIS data production is the Global 250 m Water Map (Carroll et al. 2009). The 250 m water map is derived from the Shuttle Radar Topography Mission Water Body Dataset (SWBD) and refined with a time series of MODIS water observations. The MODIS water observations are calculated as a probability of water ($\frac{\# \text{ water observations}}{\# \text{ water observation} + \# \text{ land observations}}$). Where the probability of water for a year of observations is greater than 50% and the SWBD shows water the pixel is labeled as water. Using the probability of water helps to avoid seasonal water, cloud shadows and some burn scars. For a full description of the method used to generate the 250 m water map, see Carroll et al. (2009).

The 250 m product was further defined with the additional definition of a ‘shoreline’ (defined as the last land pixel before water is encountered) and the differentiation of shallow from deep water. The global relief product ETOPO1 (<http://www.ngdc.noaa.gov/mgg/global/global.html> accessed 6 October 2010) was used to identify the depths in the water to define the categories 0, 4, 6, and 7 (Table 1). The ETOPO1 product was chosen for its global coverage and 1 arc minute spatial resolution. Depth thresholds were defined as follows: Shallow: 0–160 ft; Moderate: 161–400 ft; Deep: >400 ft to be as close to thresholds used in the original water mask as possible. Deep inland water was defined as anything deeper than 160 ft. The ephemeral water category was not populated in either the at-launch product or the C4/5 product. No attempt was made to populate the ephemeral water category for the C6 product.

Table 1. Categories represented in the multi-class water mask for MODIS.

Value	Category
0	Shallow ocean
1	Land
2	Shoreline
3	Inland water
4	Deep inland water
5	Ephemeral water (not in use)
6	Moderate ocean
7	Deep ocean

Initially, the global 250 m water map was aggregated to 500 m spatial resolution using exact averaging with the following assumptions:

- (1) There are exactly four 250 m pixels in one 500 m pixel assuming that all projection parameters remain constant.
- (2) If two or more 250 m pixels were identified as water the 500 m pixel was labeled as water.

There is a substantial difference in spatial resolution between the MODIS data (~15 arc seconds) and the ETOPO1 data (60 arc seconds). An algorithm was developed and implemented that used the spatial relationship utilities in a Geographic Information System to merge the data sets and maintain the finer resolution class boundaries.

The previous steps were automated and used to produce the initial result. Each of the 326 MODIS land tiles were then opened and evaluated by comparing against visible imagery. Tiles with apparent anomalies were identified for further evaluation. The primary anomaly identified were 'slivers', classified as 'water' from the original binary classification, between shoreline and shallow ocean that were not captured in the automated error checking. These occurred in less than 10% of the tiles and were manually converted to the shallow ocean category.

3. Results

The product generated from this work is natively in MODIS Sinusoidal grid and tiling scheme (http://modis-land.gsfc.nasa.gov/MODLAND_grid.html) and available at 500 m spatial resolution (Figure 1). To fulfill the needs of the production team, an additional product was generated that is a global depiction of the result in Latitude/Longitude (Geographic) projection on WGS-84 datum.

Some of the fine details seen in the 250 m product have been lost due to the coarsening of the spatial resolution but overall the spatial fidelity remains good (Figures 2 and 3). The continuity of rivers is lost when the width of the river is less than 500 m which is expected and is simply a constraint of the 500 m spatial resolution.

The Land Data Operational Product Evaluation team evaluated the new C6 land/water mask by comparing with the C4/5 land/water mask. Results of that evaluation are available online (http://landweb.nascom.nasa.gov/cgi-bin/QA_WWW/newPage.cgi?fileName=C6_waterMask_250m). A confusion matrix showing areas of agreement and disagreement was created and is shown in Table 2. The overall agreement on a global scale is nearly 94%, however disagreement in specific

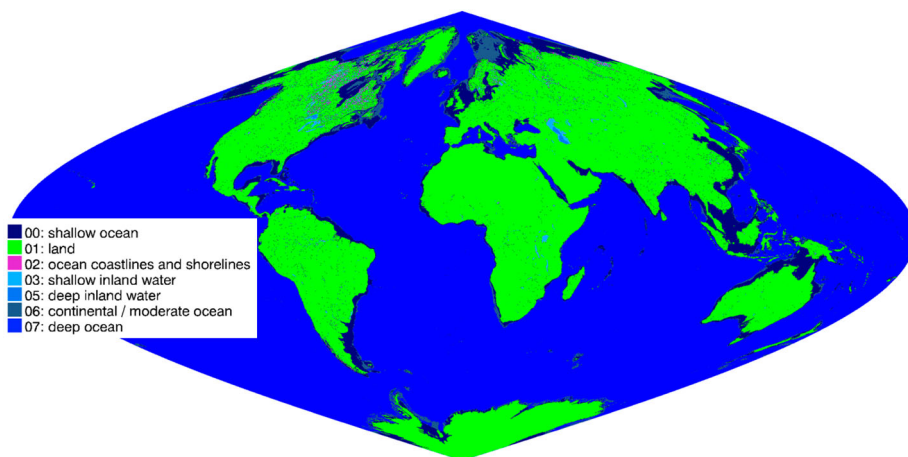


Figure 1. Global eight category water mask at 500 m resolution for the MODIS C6 data reprocessing.

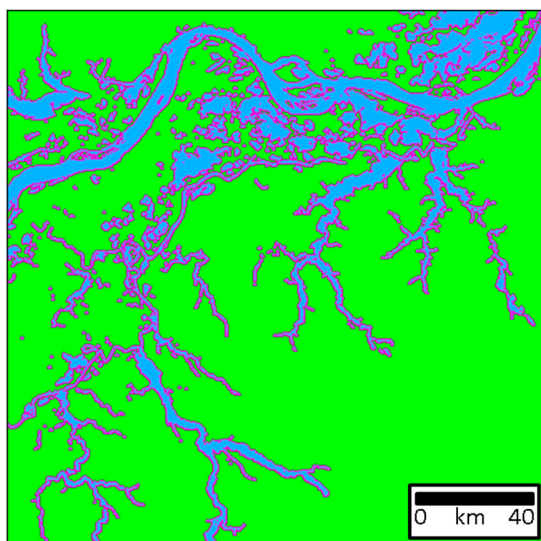


Figure 2. Amazon River, Brazil South America.

classes does occur. The 500 m C6 mask shows 2.33% of the continental surface as water (inland lakes, ponds, reservoirs, and rivers) compared to 1.45% represented as water in the C5 mask. For the shallow inland water class, there is 41% agreement between the two masks. Nearly 38% of the pixels identified as shallow inland water in the C6 mask were previously identified as 'land' in the C5 mask. If we consider land and shoreline together, 54% of the pixels identified as shallow inland water in the C6 mask were previously identified as land or shoreline in the C5 mask. This difference can be credited to the substantial difference in spatial resolution between the C5 mask (1 km) and the underlying 250 m MODIS water map. Primary areas of difference in inland water occur in the high northern latitudes where two factors result in more water being identified.

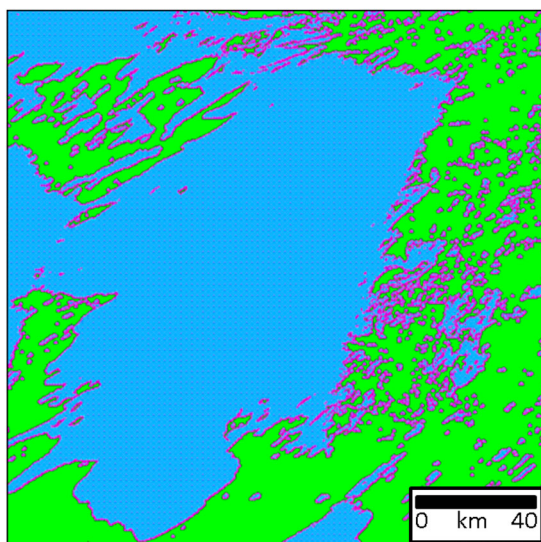


Figure 3. Large and small lakes in Canada North America.

Table 2. Confusion matrix comparing C5 vs. C6 water mask. Class 4, Ephemeral water, is not populated in either mask so has been omitted from the table.

C6 Mask	C5 Mask	0 Shallow ocean	1 Land	2 Shoreline	3 Shallow inland	5 Deep inland	6 Mod. ocean	7 Deep ocean	Total
0	Shallow ocean	66,064,777	2,494,034	3,179,627	165,235	809	45,889,107	956,637	118,750,226
1	Land	541,970	646,883,341	4,862,811	1,204,525	8095	16,423	192	653,517,357
2	Shoreline	545,582	12,370,392	2,519,087	895,621	984	6010	379	16,338,055
3	Shallow inland	72,016	5,411,904	2,366,318	5,893,698	623,283	43	–	14,367,262
5	Deep inland	123	558	915	614,639	245,001	–	–	861,236
6	Mod. ocean	5,270,037	86,763	211,545	3962	–	36,370,514	7,586,840	49,529,661
7	Deep ocean	1,814,187	5,129	12,196	57	–	7,549,884	836,966,734	846,348,187
	Total	74,308,692	667,252,121	13,152,499	8,777,737	878,172	89,831,981	845,510,782	

- (1) Improved spatial resolution from 1 km (C4/5) to 500 m (C6) result in more lakes and narrow rivers identified in the new C6 mask.
- (2) An error in the projection software resulted in a substantial shoreline shift in the C4/5 product that was corrected in the C6 product.

Delineation of shoreline is also different between the C5 mask and the new C6 mask. Nearly 5% of the pixels identified as 'shallow ocean' were previously identified as either land or shoreline. The impact of using the ETOPO1 bathymetry data set can be seen in the delineations between shallow, moderate, and deep ocean. The C6 mask shows 38% more pixels as shallow ocean when compared to the C5 mask. The majority of the reclassified values come from the moderate ocean class. There are some differences at the intersection of deep ocean and moderate ocean but these differences represent less than 1% change from C5 to C6.

A map showing the density of 'differences' between the two maps is shown in [Figure 4](#). High concentrations of change can be seen to the west of Hudson Bay in the Canadian Shield as well as along the coastlines.

4. Validation

The MODIS 250 m water map (Carroll et al. 2009) has been validated and published. The 500 m water map that is the topic of this article is a direct derivation of the finer resolution product. The stated accuracy of the 250 m water map is 98% producer's accuracy (i.e. 2% commission error) and 79% user's accuracy (i.e. 21% omission error). The majority of water bodies that are missed by the 250 m water map are small (i.e. one 250 m pixel or smaller) based on comparison with a local data set at 30 m spatial resolution (Carroll et al. 2009). Explicit validation of the 500 m product would be redundant and was not performed here.

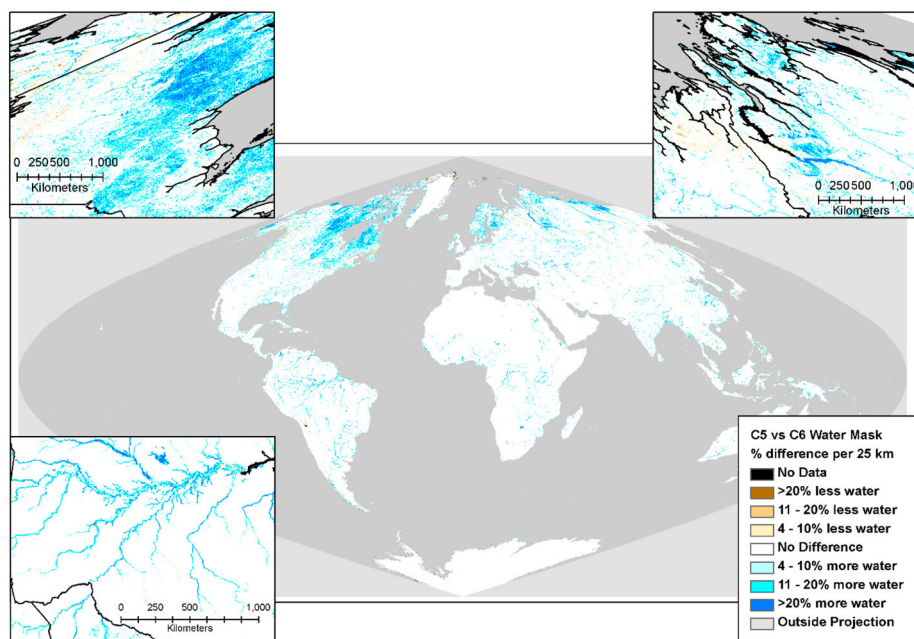


Figure 4. The differences between the C5 vs. the C6 water mask for MODIS.

Note: Differences are represented as percent difference per 25 km grid cell for visibility with more water in C6 shown in shades of blue and less water shown in shades of brown.

5. Impact of new water mask on data products

The water mask is used by product algorithms in two ways: (1) as a decision tool to allow the algorithm to process data in a different way and (2) as a mask of water applied as a post processing step to show the location of water. The MOD04 (Aerosol) and MOD11 (LST) products use the mask to decide which algorithm pathway to apply with different algorithms for land and water. The MOD44B (Vegetation Continuous Fields) and MOD13 (NDVI) products use the water mask as a mask during post processing to designate the location and extent of water.

5.1. MOD04 aerosol product

In the standard MOD04/MYD04 MODIS aerosol products, three algorithms are employed to determine the mid-visible aerosol optical depth (AOD), known as Deep Blue (DB), Dark Target (DT), and 'ocean' (although the ocean algorithm is applied over all water-covered surfaces, not just oceans). The AOD output data are provided at nominal $10 \times 10 \text{ km}^2$ resolution; $3 \times 3 \text{ km}^2$ products are also available for DT and the ocean algorithm. These algorithms take different approaches, based on the underlying surface type, due to the very different reflective behaviors of different surfaces. DB works based on the principle that the land surface reflectance at short blue wavelengths (412 nm) is typically low, leading to a contrast between clean and aerosol-laden atmospheres in this band (Hsu et al. 2013). DT provides retrievals over dark vegetated surfaces, using the principle that over these surface types the surface contribution to the signal in visible wavelengths can be estimated from the observed reflectance at the $2.1 \mu\text{m}$ MODIS band, at which the atmospheric contribution to the signal is small (Levy et al. 2007). The ocean algorithm works on the principle that the water surface at visible, near-infrared, and shortwave infrared wavelengths is dark and can be modelled with auxiliary knowledge of the near-surface wind speed (Tanré et al. 1997). The DB and DT algorithms have been validated and have similar levels of uncertainty. The uncertainty on over-water retrievals is somewhat smaller (Levy et al. 2013; Sayer et al. 2013, 2014; Sayer, Hsu, and Bettenhausen 2015). DT discards pixels defined by MOD03 (geolocation) as coastal/shore (and attempts no AOD retrieval if the whole $10 \times 10 \text{ km}^2$ retrieval box falls into this category), while DB treats these as land pixels.

As noted in Levy et al. (2013) and shown in Figure 4, one of the regions affected by the updated land mask in MODIS C6 is high latitudes in North America and Asia, which contain many small lakes. The MODIS C6 water mask identifies a larger proportion of water-covered pixels at 500 m, which leads to more $10 \times 10 \text{ km}^2$ retrieval boxes identified as coastal (i.e. no retrieval) or water surfaces by the DT algorithm. This has implications for AOD data coverage and quality, as shown in Figure 5 which illustrates a MODIS granule covering parts of the USA and Canada near Lake Superior.

The C6 water mask from MOD03 (Figure 5(b)) identifies many pixels as coastal, due to sub-pixel water content (at the 1 km level). Comparing the C5–C6 algorithm decision trees (panels c, d), many formerly 'land' pixels are now entirely 'coastal', meaning that coverage is lost in the AOD data (panels f, g). In contrast, pixels on the edges of Lakes Superior and Nipigon are more accurately identified as land or water, increasing coverage of AOD in C6 here. The 3 km data set is also shown, with similar features to the 10 km data.

Also of note, many of the AOD values retrieved were zero or negative in C5. Although negative AOD is out of physical bounds for the parameter, small negative values are permitted by the DT retrieval for statistical purposes (Levy et al. 2007). These negative AOD retrievals occur in the data here in part because the retrieval algorithm was assuming a land surface when in fact many of the pixels averaged for the retrieval were water-covered, and thus darker than assumed by the land surface model. This resulting high bias in assumed surface reflectance translates to out of bounds negative AOD values. In C6, although spatial coverage is smaller, the improved land mask means that the DT algorithm is able to more accurately identify which pixels correspond to

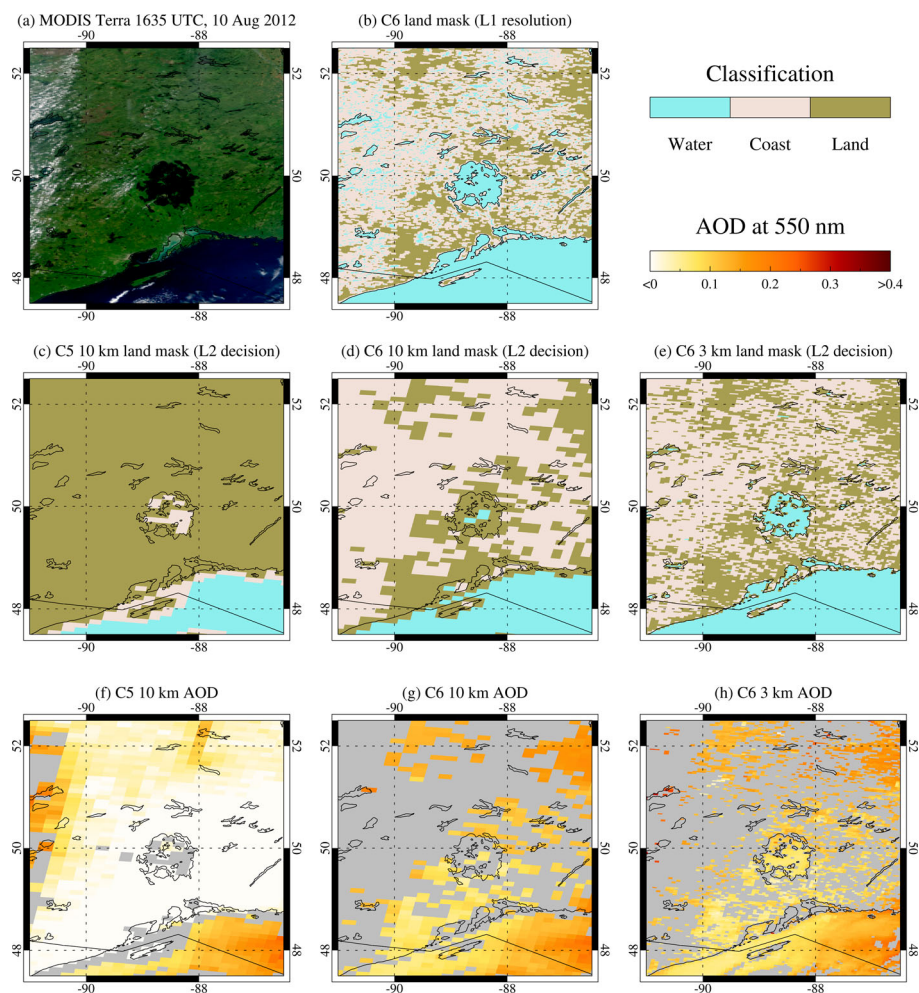


Figure 5. Effect of improved land mask on MODIS DT/ocean aerosol retrievals in areas of small lakes. Panel (a) shows a true-color MODIS Terra image, and (b) the MOD03 land mask used as input to the aerosol retrieval algorithms. Panels (c–e) show the land/water decision for the C5, C6, and 3 km C6 data products (based on the land mask at full MODIS resolution). Panels (f–h) show the resulting AOD retrievals at 550 nm.

Note: Pixels without valid AOD retrievals are shaded in grey.

land, water, or mixed surfaces, meaning only suitable pixels are used for the respective algorithms, greatly mitigating the potential for this bias. For this particular scene, the Aerosol Robotic Network (Holben et al. 1998) mid-visible AOD for the site at Pickle Lake (51.4° N, 90.1° W) was ~ 0.25 , in close agreement with nearby C6 values. Thus, the updated water mask improves the AOD retrieval in areas of sub-pixel (on a 1 km scale) water coverage.

5.2. MOD11 LST

The MOD11 LST algorithm uses a split-window approach with the 1 km thermal bands on MODIS data from both the Terra and Aqua platforms (Coll and Caselles 1997; Wan and Dozier 1996; Wan and Li 2011) to produce the LST product. This algorithm uses the emissivity measured in the thermal infrared bands to determine the temperature of the land surface. Information about the atmosphere at the time of acquisition, including water vapor pressure, is also required to perform the

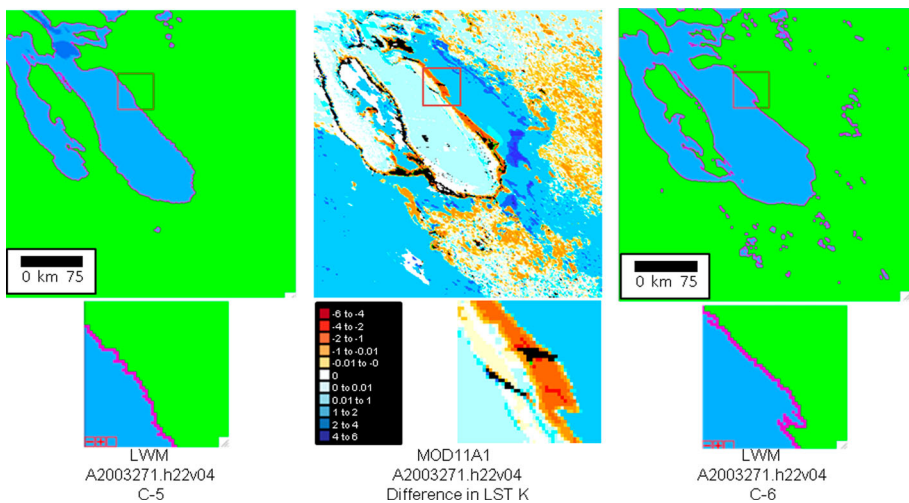


Figure 6. Land water mask for C5 and C6 for the Aral Sea and the difference in LST for data day 2,003,271 from C5 and C6. Temperatures differ by ~ 4 K where the water mask has changed between the two data collections.

calculations. The water vapor profile is estimated in the MOD07 product and used to calculate LST. Emissivity is more easily calculated over uniform surfaces such as water, hence the land/water mask is used to provide *a-priori* information about the land surface prior to applying the algorithm.

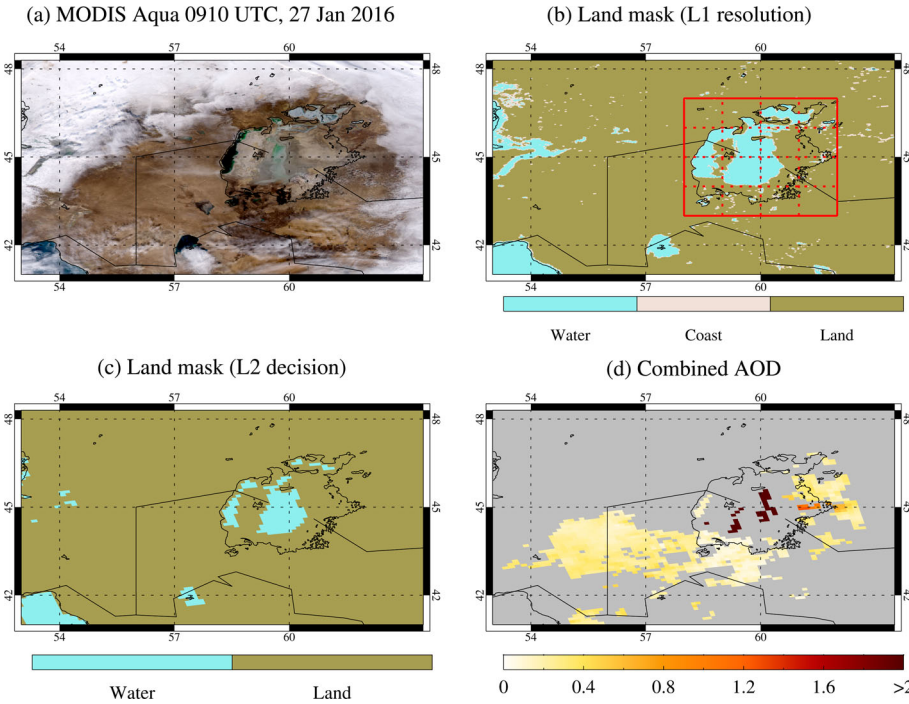


Figure 7. Effect of a static land mask on MODIS aerosol retrievals around the Aral Sea. Panel (a) shows a true-color MODIS Aqua image, (b) the input MOD03 land mask, and (c) the land/water decision at the nominal MODIS 10 km pixel size. The red grid in panel (b) indicates the areas for the time series analysis shown in Figure 8. Panel (d) illustrates the retrieved AOD at 550 nm (in this case, from the water algorithm for areas identified as water in panel c, and from DB in panel d), after cloud masking and QA steps.

Note: Pixels without valid AOD retrievals are shaded in grey. Note the coastline drawn represents the 1960s Aral Sea coastline.

With significantly more water pixels represented in the MODIS C6 water mask there were more pixels in the LST product that were processed with the simple radiance calculation (used over water) rather than the split-window technique. This is evident in Figure 6 showing the difference between Collection 5 (C5) and C6 LST over the Aral Sea.

6. More work to be done

As noted earlier, water is not a static land cover type and in some cases can be particularly transient. Rivers meander and salt pans in Africa and Australia can fill for a month or more and then be dry for the rest of the year. In other cases such as the Aral Sea there is a well-documented long-term decline in surface area with human and environmental consequences (Micklin 2007). The Salton Sea of Southern California is showing similar impacts as it is slowly starved of recharge. These cases have an impact on the performance of algorithms such as the MOD04 aerosol product because the area flagged as water in the static water mask that was correct at the time of the water mask creation is not accurate at a later time. This results in inaccuracies in the aerosol data where the ‘ocean’ algorithm is used when one of the land algorithms (i.e. DB or DT) should have been used because there is actually no water in the pixel. This is problematic for an individual date as illustrated by Figure 7, but is worse when evaluated as a time series as illustrated in Figure 8, since the long-term decline in water coverage results in an artificial trend in AOD in this region. To address this two steps are needed. First, an annual water map with an ephemeral water class needs to be created. Second, algorithms such as the MOD04 aerosol need to be modified to consider the changing area of surface water.

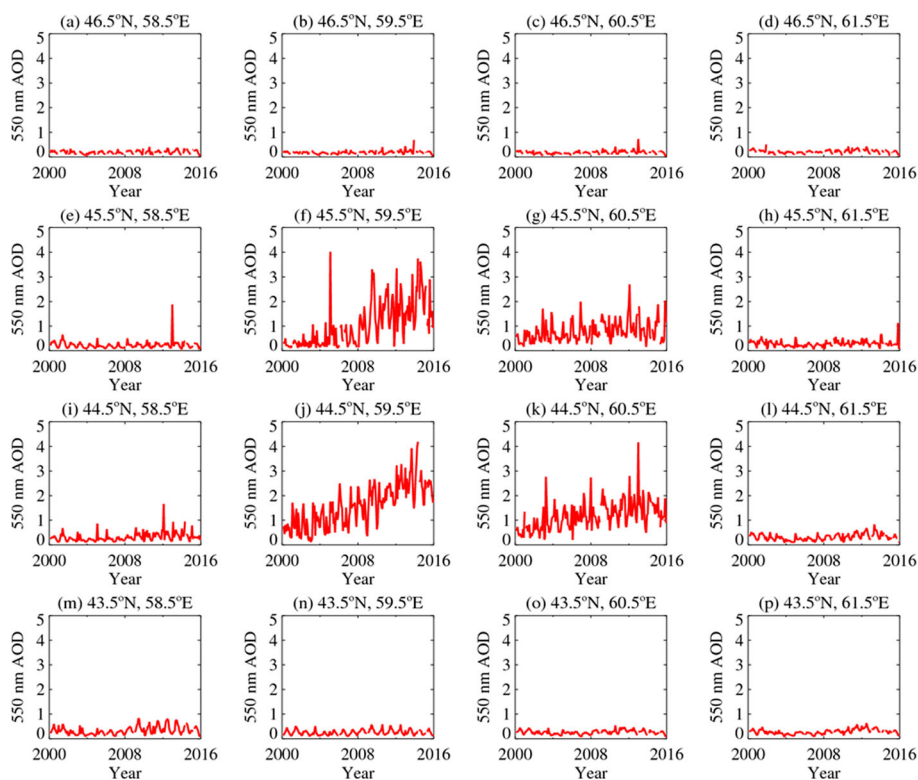


Figure 8. Time series of monthly mean AOD from MODIS Terra, for 1° grid cells indicated in Figure 7(b).

Note: Panel titles indicate the central latitude/longitude of each grid cell, and panels are arranged geographically.

7. Conclusions

The C6 land/water mask represents a substantial improvement in accuracy in the representation of water for the MODIS data processing stream. We have demonstrated some of the impacts to downstream products that use the land/water mask in algorithm pathway logic (i.e. algorithms that operate one way if it is land and a different way if it is water) and have shown some examples of these impacts. The local and regional impacts are significant in some regions such as the Canadian Shield where more areas are now identified as water. This water mask is implemented in the level 1 geolocation product (MOD03) for MODIS and hence has an impact on all products from Land, Atmospheres and Oceans which use the L1B as input to downstream processes. We have shown the impact of the C6 water mask on the MOD04 aerosol and MOD11 LST products. Future improvements should include annually updated water maps that take into consideration ephemeral water.

Acknowledgements

The authors would like to thank the MODIS Land Science Team for their continuing support of this effort. The authors would also like to thank the journal editors and anonymous reviewers.

Disclosure statement

No potential conflict of interest was reported by the authors.

Funding

This work was funded in part by National Aeronautics and Space Administration (NASA) Terrestrial Ecology program Grant/Cooperative Agreement Number: #NNX08AT97A; NASA MEaSURES program Grant/Cooperative Agreement Number: #NNX13AJ35A; and NASA EOS Grant/Cooperative Agreement Number: #NNX14AJ33G.

ORCID

A. I. Elders  <http://orcid.org/0000-0001-7706-1846>

S. Devadiga  <http://orcid.org/0000-0003-4300-3351>

References

- Carroll, M. L., J. R. Townshend, C. M. DiMiceli, P. Noojipady, and R. A. Sohlberg. 2009. "A New Global Raster Water Mask at 250 m Resolution." *International Journal of Digital Earth* 2: 291–308.
- Coll, C., and V. Caselles. 1997. "A Split-Window Algorithm for Land Surface Temperature from Advanced Very High Resolution Radiometer Data: Validation and Algorithm Comparison." *Journal of Geophysical Research: Atmospheres* 102: 16697–16713.
- Holben, B. N., T. F. Eck, I. Slutsker, D. Tanré, J. P. Buis, A. Setzer, E. Vermote, et al. 1998. "AERONET – A Federated Instrument Network and Data Archive for Aerosol Characterization." *Remote Sensing of Environment* 66: 1–16.
- Hsu, N. C., M.-J. Jeong, C. Bettenhausen, A. M. Sayer, R. Hansell, C. S. Seftor, J. Huang, and S. C. Tsay. 2013. "Enhanced Deep Blue Aerosol Retrieval Algorithm: The Second Generation." *Journal of Geophysical Research: Atmospheres* 118: 9296–9315.
- Justice, C. O., J. R. G. Townshend, E. F. Vermote, E. Masuoka, R. E. Wolfe, N. Saleous, D. P. Roy, and J. T. Morisette. 2002. "An Overview of MODIS Land Data Processing and Product Status." *Remote Sensing of Environment* 83: 3–15.
- Levy, R. C., S. Mattoo, L. A. Munchak, L. A. Remer, A. M. Sayer, F. Patadia, and N. C. Hsu. 2013. "The Collection 6 MODIS Aerosol Products Over Land and Ocean." *Atmospheric Measurement Techniques* 6: 2989–3034.
- Levy, R. C., L. A. Remer, S. Mattoo, E. F. Vermote, and Y. J. Kaufman. 2007. "Second-Generation Operational Algorithm: Retrieval of Aerosol Properties Over Land from Inversion of Moderate Resolution Imaging Spectroradiometer Spectral Reflectance." *Journal of Geophysical Research: Atmospheres* 112: D13211.
- Masuoka, E., D. P. Roy, R. Wolfe, J. T. Morisette, S. Sinno, M. Teague, N. Saleous, S. Devadiga, C. Justice, and J. Nickeson. 2011. "MODIS Land Data Products: Generation, Quality Assurance and Validation." In *Land Remote*

- Sensing and Global Environmental Change*, edited by B. Ramachandran, C. Justice, and M. Abrams, 509–531. New York: Springer.
- Micklin, P. 2007. “The Aral Sea Disaster.” *Annual Review of Earth and Planetary Sciences* 35: 47–72.
- Salomon, J., J. Hodges, M. Friedl, C. Schaaf, A. Strahler, F. Gao, A. Schneider, X. Zhang, N. El Saleous, and R. Wolfe. 2004. “Global Land-Water Mask Derived from MODIS Nadir BRDF-Adjusted Reflectances (NBAR) and the MODIS Land Cover Algorithm.” Geoscience and remote sensing symposium. IGARSS ‘04. Proceedings. 2004 IEEE International, Alaska, September 20–24, 2004, 241.
- Sayer, A. M., N. C. Hsu, and C. Bettenhausen. 2015. “Implications of MODIS Bow-Tie Distortion on Aerosol Optical Depth Retrievals, and Techniques for Mitigation.” *Atmospheric Measurement Techniques* 8: 5277–5288.
- Sayer, A. M., N. C. Hsu, C. Bettenhausen, and M.-J. Jeong. 2013. “Validation and Uncertainty Estimates for MODIS Collection 6 ‘Deep Blue’ Aerosol Data.” *Journal of Geophysical Research: Atmospheres* 118: 7864–7872.
- Sayer, A. M., L. A. Munchak, N. C. Hsu, R. C. Levy, C. Bettenhausen, and M.-J. Jeong. 2014. “MODIS Collection 6 Aerosol Products: Comparison Between Aqua’s E-Deep Blue, Dark Target, and ‘Merged’ Data Sets, and Usage Recommendations.” *Journal of Geophysical Research: Atmospheres* 119: 13965–13989.
- Tanré, D., Y. J. Kaufman, M. Herman, and S. Mattoo. 1997. “Remote Sensing of Aerosol Properties Over Oceans Using the MODIS/EOS Spectral Radiances.” *Journal of Geophysical Research: Atmospheres* 102: 16971–16988.
- Wan, Z. M., and J. Dozier. 1996. “A Generalized Split-Window Algorithm for Retrieving Land-Surface Temperature from Space.” *IEEE Transactions on Geoscience and Remote Sensing* 34: 892–905.
- Wan, Z., and Z.-L. Li. 2011. “Chapter 25. MODIS Land Surface Temperature and Emissivity.” In *Land Remote Sensing and Global Environmental, NASA’s Earth Observing System and the Science of ASTER and MODIS*, edited by C. O. J. B. Ramachandran and M. J. Abrams, 563–577. New York: Springer.